

Article

High-Level Bio-Based Production of Coproporphyrin in *Escherichia coli*

Bahareh Arab, Adam Westbrook, Murray Moo-Young, Yilan Liu and C. Perry Chou * 

Department of Chemical Engineering, University of Waterloo, Waterloo, ON N2L 3G1, Canada

* Correspondence: cpchou@uwaterloo.ca; Tel.: +1-519-888-4567 (ext. 33310)

Abstract: This study reports on the development of effective strain engineering strategies for the high-level bio-based production of coproporphyrin (CP), a porphyrin pigment compound with various applications, using *Escherichia coli* as a production host. Our approach involves heterologous implementation of the Shemin/C4 pathway in an *E. coli* host strain with an enlarged intracellular pool of succinyl-CoA. To regulate the expression of the key pathway genes, including *hemA/B/D/E/Y*, we employed a plasmid system comprising two operons regulated by strong *trc* and *gracmax* promoters, respectively. Using the engineered *E. coli* strains for bioreactor cultivation under aerobic conditions with glycerol as the carbon source, we produced up to 353 mg/L CP with minimal byproduct formation. The overproduced CP was secreted extracellularly, posing minimal physiological toxicity and impact on the producing cells. To date, targeted bio-based production of CP by *E. coli* has yet to be reported. In addition to the demonstration of high-level bio-based production of CP, our study underscores the importance of identifying key enzymatic reactions limiting the overall metabolite production for developing differential expression strategies for pathway modulation and even optimization. This investigation paves the way for the development of effective metabolic engineering strategies based on targeted manipulation of key enzymes to customize engineered strains for effective large-scale bio-based production.

Keywords: batch bioreactor; coproporphyrin; *Escherichia coli*; metabolic engineering; Shemin/C4 pathway; synthetic biology



Citation: Arab, B.; Westbrook, A.; Moo-Young, M.; Liu, Y.; Chou, C.P. High-Level Bio-Based Production of Coproporphyrin in *Escherichia coli*. *Fermentation* **2024**, *10*, 250. <https://doi.org/10.3390/fermentation10050250>

Academic Editor: Mohamed Koubaa

Received: 16 April 2024

Revised: 5 May 2024

Accepted: 8 May 2024

Published: 11 May 2024



Copyright: © 2024 by the authors. Licensee MDPI, Basel, Switzerland. This article is an open access article distributed under the terms and conditions of the Creative Commons Attribution (CC BY) license (<https://creativecommons.org/licenses/by/4.0/>).

1. Introduction

Heme is an essential compound in various hemoproteins, such as hemoglobin, myoglobin, and cytochromes, and plays a critical role in oxygen transportation, energy generation, and several enzymatic activities [1]. In bacteria, heme can be naturally synthesized via two distinct pathways: i.e., protoporphyrin-dependent (PPD) and coproporphyrin-dependent (CPD) pathways [2], with the PPD pathway being predominantly present in Gram-negative bacteria and the CPD pathway in Gram-positive bacteria [3]. In both pathways, heme biosynthesis starts with the formation of 5-aminolevulinic acid (5-ALA) via either the C4 or C5 pathway [4] (Figure 1). Subsequently, the enzyme porphobilinogen synthase (HemB) mediates the fusion of two 5-ALA molecules, yielding porphobilinogen (PBG). Then, PBG deaminase (HemC) interconnects and cyclizes four PBG molecules to form a linear tetrapyrrole, hydroxymethylbilane (HMB) [5]. At this metabolic node, the heme biosynthetic pathway diverges to form either of the two stereoisomers, i.e., uroporphyrinogen I (UPG-I) via autoxidation or uroporphyrinogen III (UPG-III) via uroporphyrinogen III synthase (HemD). Uroporphyrinogen decarboxylase (HemE) decarboxylates the four acetate residues of UPG-I to form coproporphyrinogen I (CPG-I), which is spontaneously oxidized to form coproporphyrin I (CP-I) as a metabolic end product [6]. Similarly, HemE mediates the conversion of UPG-III to coproporphyrinogen III (CPG-III), which is enzymatically converted to coproporphyrin III (CP-III) via coproporphyrinogen III oxidase (HemY) or porphyrinogen peroxidase (YfeX). Note that CPG-III represents the final shared

precursor in the PPD and CPD pathways, both of which lead to the formation of heme via its respective precursors of protoporphyrin IX (PP-IX) and CP-III.

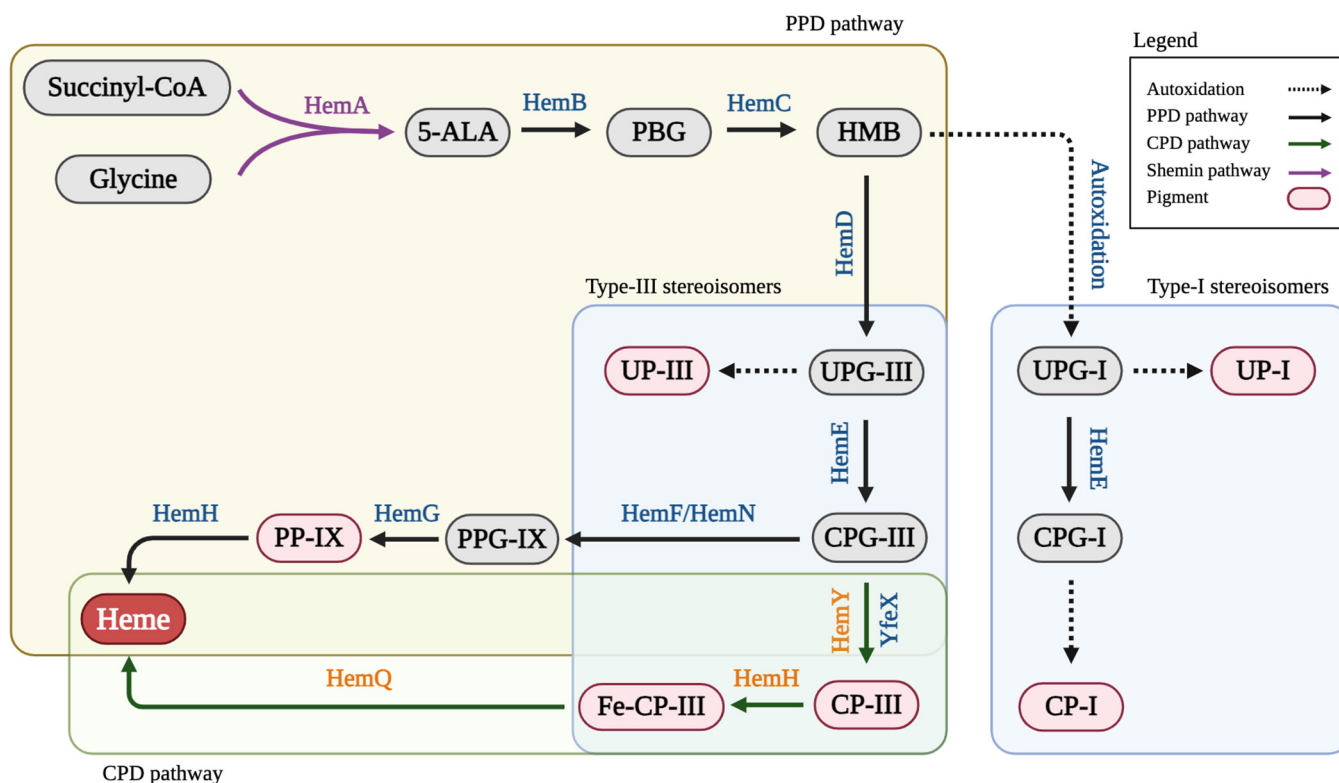


Figure 1. The Shemin/C4 pathway for porphyrin biosynthesis from succinyl-CoA and glycine. 5-ALA, 5-aminolevulinic acid; CPG-I, coproporphyrinogen I; CPG-III, coproporphyrinogen III; CP-I, coproporphyrin I; CP-III, coproporphyrin III; Fe-CP-III, coproheme III; HemA, 5-aminolevulinatase synthase; HemB, porphobilinogen synthase; HemC, porphobilinogen deaminase; HemD, uroporphyrinogen III synthase; HemE, uroporphyrinogen decarboxylase; HemF, coproporphyrinogen III oxidase; HemG, protoporphyrinogen oxidase; HemH, protoporphyrin/coproporphyrin ferrochelatase; HemN, oxygen-independent coproporphyrinogen III oxidase; HemQ, coproheme decarboxylase; HemY, coproporphyrinogen III oxidase; HMB, Hydroxymethylbilane; PBG, porphobilinogen; PP-IX, protoporphyrin IX; PPG-IX, protoporphyrinogen IX; UP-I, uroporphyrin I; UP-III, uroporphyrin III; UPG-I, uroporphyrinogen I; UPG-III, uroporphyrinogen III; YfeX, porphyrinogen peroxidase.

Porphyrin production in microbial hosts presents a sustainable and economically feasible alternative to traditional chemical synthesis methods, particularly in light of the growing demand for bio-based production strategies [7]. Modulating the metabolic capabilities of microorganisms, notably the most common bacterial host, *Escherichia coli*, facilitates the efficient and sustainable synthesis of porphyrins [8]. The well-characterized genetics and versatile metabolic engineering tools enable precise regulation of biosynthetic pathways in *E. coli* [9]. Given the commercial value and applicability of heme, its bio-based production has been explored [10]. While *E. coli* can be extensively engineered for enhanced heme biosynthesis, the overproduced heme is hard to secrete and tends to accumulate intracellularly, resulting in physiological toxicity to the production host and, therefore, limited production yield [11,12]. Such technical limitation prompted us to look for alternative porphyrins that could be extracellularly secreted for overproduction in *E. coli*.

Coproporphyrin (CP), specifically CP-III, is a critical porphyrin intermediate and precursor for heme biosynthesis via the CPD pathway [13]. Beyond its significance in heme biosynthesis, CP holds noteworthy applications across diverse fields. Derivatives of CP are pivotal in clinical diagnostics such as the diagnosis of porphyria [14]. CP can also serve

as a diagnostic biomarker [15,16]. Moreover, due to unique optical properties and low cytotoxicity, CP has applications beyond healthcare, including use as fluorescent probes, in photodynamic therapy, and as bioimaging agents [17–19].

In *E. coli*, the PPD pathway is primarily used for heme biosynthesis (Figure 1). However, the simultaneous presence of enzymes and pathways diverging from the PPD pathway offers potential opportunities for the biosynthesis of porphyrins other than heme. Given the above-mentioned technical limitation associated with intracellular accumulation of heme, we herein focused on CP for its bio-based production in *E. coli*. While minimal CP production was observed in our previous study [20], it is noteworthy that targeted bio-based CP production in *E. coli* has yet to be reported. Note that the overproduced CP can be further processed, either chemically or biochemically, to form heme. In this study, we first heterologously implemented the Shemin/C4 pathway in an *E. coli* host strain with an expanded intracellular pool of succinyl-CoA, a key precursor for porphyrin biosynthesis via the Shemin/C4 pathway. Considering the complexity of the pathway and enzymes involved in CP biosynthesis, differential expression strategies for modulation of the levels of key enzymes, particularly those governing the sequential conversion of 5-ALA to CP, were applied as a strategic metabolic approach for enhanced CP biosynthesis in *E. coli*. Selective alteration of key enzyme levels enabled fine-tuning of the associated metabolic flux in the CP biosynthetic pathway, optimal substrate channeling, and minimal accumulation of intermediates or byproducts. Moreover, by applying differential expression strategies, we can minimize the metabolic burden imposed by enzyme overexpression, ensuring efficient utilization of cellular resources to increase product yield [21]. By exploring diverse combinations of specific pathway genes for heterologous expression, we developed a flexible platform to engineer *E. coli* strains for high-level CP biosynthesis under aerobic conditions using glycerol as the primary carbon source.

2. Materials and Methods

2.1. Bacterial Strains and Plasmids

The bacterial strains and plasmids used in this study are provided in Table 1, and the primer sequences are listed in Table S1. Taq DNA polymerase was obtained from New England Biolabs (Ipswich, MA, USA). Genomic DNA of the bacterial cells was extracted using the Qiagen Blood & Tissue DNA Isolation Kit (Hilden, Germany). Plasmids were purified using the Qiagen Miniprep kit. All host cells in this study were derived from CPC-Sbm through the introduction of mutation(s) in the *sdhA* and/or *iclR* genes [22]. It is noteworthy that CPC-Sbm originated from BW25113 with the *ldhA* gene inactivated [23]. For molecular cloning, *E. coli* HI-Control 10G (Lucigen, Middleton, WI, USA) was used. DNA sequencing was performed by Plasmidsaurus (Eugene, OR, USA). All plasmids were constructed through Gibson assembly [24]. All oligonucleotides were synthesized by Integrated DNA Technologies (IDT) (Coralville, IA, USA).

Plasmid pK-hemABCD was used from our previous study to serve as the template for the remaining plasmids [20]. More information is available in the Supplementary Materials. Plasmid pK-hemABCD-E was also constructed to serve as the template for the other plasmids containing two operons. pK-hemABCD-E was constructed by amplifying *hemA* along with the backbone, consisting of p15A ori and *trc* promoter with a kanamycin resistance marker, using primers P002/P011 and amplifying *hemB*, *hemC*, and *hemD* using primers P003/P012 and pK-hemABCD as a template. The *hemE* gene was amplified from the genomic DNA of *E. coli* MG1655 using primers P013/P014. The *gracmax* promoter was amplified from a previous lab-made plasmid using primers P015/P016. Subsequently, these four fragments were Gibson-assembled to form pK-hemABCD-E. For effective coexpression, *hemA*, *hemB*, *hemC*, and *hemD* were aligned to form an operon *hemA/B/C/D* regulated by a common strong *trc* promoter and *hemE* was included on the second operon regulated by the *gracmax* promoter with an individual strong ribosomal binding site (RBS) for each gene.

Table 1. Strains and plasmids used in this study.

Name	Description or Relevant Genotype	Source
Host strains		
HI-Control 10G	<i>mcrA</i> , $\Delta(mrr-hsdRMS-mcrBC)$, <i>endA1</i> , <i>recA1</i> , $\phi 80dlacZ\Delta M15$, $\Delta lacX74$, <i>araD139</i> , $\Delta(ara\ leu)7697$, <i>galU</i> , <i>galK</i> , <i>rpsL</i> (Str ^R), <i>nupG</i> , λ^- , <i>tonA</i> , Mini-F <i>lacI</i> ^{q1} (Gent ^R)	Lucigen
MG1655	K-12; F ⁻ , λ^- , <i>rph-1</i>	Lab stock
<i>Bacillus Subtilis</i> 168	Wild type	Lab stock
CPC-Sbm $\Delta iclR\Delta sdhA$	F ⁻ , $\Delta(araD-araB)567$, $\Delta lacZ4787(::rrnB-3)$, λ^- , <i>rph-1</i> , $\Delta(rhaD-rhaB)568$, <i>hsdR514</i> , ΔdhA , P _{trc} :: <i>sbm</i> (i.e., with the FRT-P _{trc} cassette replacing the 204-bp upstream of the Sbm operon), $\Delta iclR$, $\Delta sdhA$	[22]
BA001	CPC-Sbm $\Delta iclR\Delta sdhA$ /pK-hemABD	[20]
BA002	CPC-Sbm $\Delta iclR\Delta sdhA$ /pK-hemABD-E	This study
BA003	CPC-Sbm $\Delta iclR\Delta sdhA$ /pK-hemAB-DE	This study
BA004	CPC-Sbm $\Delta iclR\Delta sdhA$ /pK-hemABD-EY _{B,s}	This study
BA005	CPC-Sbm $\Delta iclR\Delta sdhA$ /pK-hemABD-EY	This study
BA006	CPC-Sbm $\Delta iclR\Delta sdhA$ /pK-hemAB-E	This study
Plasmids		
pK-hemABCD	p15A ori, Km ^R , P _{trc} :: <i>hemABCD</i>	[20]
pK-hemABCD-E	p15A ori, Km ^R , P _{trc} :: <i>hemABCD</i> -P _{gracmax} :: <i>hemE</i>	This study
pK-hemABD	p15A ori, Km ^R , P _{trc} :: <i>hemABD</i>	[20]
pK-hemABD-E	p15A ori, Km ^R , P _{trc} :: <i>hemABD</i> -P _{gracmax} :: <i>hemE</i>	This study
pK-hemAB-DE	p15A ori, Km ^R , P _{trc} :: <i>hemAB</i> -P _{gracmax} :: <i>hemDE</i>	This study
pK-hemABD-EY _{B,s}	p15A ori, Km ^R , P _{trc} :: <i>hemABD</i> -P _{gracmax} :: <i>hemEY</i> - <i>hemY</i> from <i>B. subtilis</i> 168-	This study
pK-hemABD-EY	p15A ori, Km ^R , P _{trc} :: <i>hemABD</i> -P _{gracmax} :: <i>hemEY</i> - <i>hemY</i> from MG1655-	This study
pK-hemAB-E	p15A ori, Km ^R , P _{trc} :: <i>hemAB</i> -P _{gracmax} :: <i>hemE</i>	This study

pK-hemABD was used from our previous study [20]. pK-hemABD-E was constructed by amplifying *hemA* and *hemB* using primers P001/P004 and amplifying *hemD* and *hemE* along with the backbone using primers P017/P018, using pK-hemABCD-E as a template. These two fragments were Gibson-assembled to form pK-hemABD-E. For effective coexpression, *hemA*, *hemB*, and *hemD* were aligned to form an operon *hemA/B/D* regulated by a common strong *trc* promoter and *hemD* was included on the second operon regulated by the *gracmax* promoter with an individual strong RBS for each gene.

pK-hemAB-DE was constructed by amplifying *hemA* and *hemB* using primers P001/P019 and pK-hemABCD as a template. *gracmax* promoter and *hemD* were amplified from pK-hemABD-E separately using primer sets P020/P021 and P022/P023, respectively. *hemE* was amplified along with the backbone, using primers P018/P024 and pK-hemABD-E as a template. These four fragments were Gibson-assembled to form pK-hemAB-DE. *hemA* and *hemB* were aligned to form an operon *hemA/B* regulated by a common strong *trc* promoter and *hemD/E* were included on the second operon regulated by the *gracmax* promoter with an individual strong RBS for each gene.

pK-hemABD-EY_{B,s} was constructed by amplifying *hemA*, *hemB*, *hemD*, and *hemE* using primers P001/P025 and pK-hemABD-E as a template. The *hemY* gene was amplified from the genomic DNA of *Bacillus subtilis* 168 using primers P026/P027. The backbone was amplified from pK-hemABD-E using primers P028/P029. These three fragments were Gibson-assembled to form pK-hemABD-EY_{B,s}. *hemA*, *hemB*, and *hemD* were aligned to form an operon *hemA/B/D* regulated by a common strong *trc* promoter and *hemE/Y* were

included on the second operon regulated by the *gracmax* promoter with an individual strong RBS for each gene.

pK-hemABD-EY was constructed by amplifying *hemA*, *hemB*, *hemD*, and *hemE* using primers P001/P025 and pK-hemABD-E as template. The *hemY* gene was amplified from the genomic DNA of *Escherichia coli* MG1655 using primers P030/P031. The backbone was amplified from pK-hemABD-E using primers P032/P029. These three fragments were Gibson-assembled to form pK-hemABD-EY. *hemA*, *hemB*, and *hemD* were aligned to form an operon *hemA/B/D* regulated by a common strong *trc* promoter and *hemE/Y* were included on the second operon regulated by the *gracmax* promoter with an individual strong RBS for each gene.

pK-hemAB-E was constructed by amplifying *hemA* and *hemB*, and amplifying *gracmax* promoter and *hemE* along with the backbone, using primer sets P019/P033 and P020/P034 with pK-hemABCD-E as a template. These two fragments were Gibson-assembled to form pK-hemAB-E. *hemA* and *hemB* were aligned to form an operon *hemA/B* regulated by a common strong *trc* promoter and *hemE* was included on the second operon regulated by the *gracmax* promoter with an individual strong RBS for each gene.

2.2. Media and Bacterial Cell Cultivation

All medium components were obtained from Sigma-Aldrich Co. (St. Louis, MO, USA), with the exception of yeast extract and tryptone, which were obtained from BD Diagnostic Systems (Franklin Lakes). *E. coli* strains were preserved as glycerol stocks at $-80\text{ }^{\circ}\text{C}$ and streaked on lysogeny broth (LB; 10 g/L tryptone, 5 g/L yeast extract, and 5 g/L NaCl) agar plates, then incubated at $37\text{ }^{\circ}\text{C}$ for 14–16 h. Bioreactor cultivations were conducted following the methodology outlined in our prior research [20]. Briefly, for bioreactor cultivation, individual single colonies were picked from LB plates to inoculate 12 mL of super broth (SB) medium (32 g/L tryptone, 20 g/L yeast extract, and 5 g/L NaCl) in a 125 mL conical flask. The culture was incubated at $37\text{ }^{\circ}\text{C}$ and 280 revolutions per min (rpm) using a rotary shaker (New Brunswick Scientific, Edison Township, NJ, USA) for 4–6 h and subsequently used as a starter culture to inoculate 220 mL of SB medium at a 2% (vol/vol) concentration in a 1 L conical flask. The seed culture was incubated at $37\text{ }^{\circ}\text{C}$ and 280 rpm for 14–16 h. Cells were harvested by centrifugation at $4500\times g$ and $20\text{ }^{\circ}\text{C}$ for 8 min and resuspended in 40 mL of fresh SB medium. The resuspended culture was used to inoculate a stirred tank bioreactor (BioFlo 115, Eppendorf AG, Hamburg, Germany) with a working volume of 0.8 L at $37\text{ }^{\circ}\text{C}$ and 430 rpm. The semi-defined production medium in the batch bioreactor contained 30 g/L glycerol, 0.23 g/L K_2HPO_4 , 0.51 g/L NH_4Cl , 49.8 mg/L MgCl_2 , 48.1 mg/L K_2SO_4 , 1.52 mg/L FeSO_4 , 0.055 mg/L CaCl_2 , 2.93 g/L NaCl, 0.72 g/L tricine, 10 g/L yeast extract, 10 mM NaHCO_3 , and 1 mL/L trace elements (2.86 g/L H_3BO_3 , 1.81 g/L $\text{MnCl}_2\cdot 4\text{H}_2\text{O}$, 0.222 g/L $\text{ZnSO}_4\cdot 7\text{H}_2\text{O}$, 0.39 g/L $\text{Na}_2\text{MoO}_4\cdot 2\text{H}_2\text{O}$, 79 $\mu\text{g/L}$ $\text{CuSO}_4\cdot 5\text{H}_2\text{O}$, 49.4 $\mu\text{g/L}$ $\text{Co}(\text{NO}_3)_2\cdot 6\text{H}_2\text{O}$); (Neidhardt, Bloch, and Smith, 1974), supplemented with 0.05 mM isopropyl β -D-1-thiogalactopyranoside (IPTG). To avoid glycine limiting during the cultivation, 2 g of glycine was supplemented into the bioreactor ~ 30 h post inoculation. The aerobic condition was maintained by continuously purging the air into the bulk culture at 1 volume of air per volume of liquid per min (vvm). The pH of the bioreactor culture was maintained at 7.0 ± 0.1 using 3 M NH_4OH and 3 M H_3PO_4 .

2.3. Analysis

To measure cell density at OD600, all culture samples were washed once and then appropriately diluted with a 0.15 M saline solution and analyzed using a spectrophotometer (GENESYSTM 40/50 Vis/UV-Vis, Thermo Fisher Scientific Inc., Waltham, MA, USA). To prepare a cell-free medium, culture samples were centrifuged at $17,000\times g$ for 1 min, followed by filter sterilization using a 0.2 μm syringe filter. Extracellular metabolites and glycerol were analyzed by high-performance liquid chromatography (HPLC; LC-10AT; Shimadzu, Kyoto, Japan) with a refractive index detector (RID; RID-10A; Shimadzu) and a chromatographic column (Aminex HPX-87H; Bio-Rad Laboratories, Hercules, CA, USA).

The HPLC column temperature was maintained at 35 °C and the mobile phase was 5 mM H₂SO₄ (pH 2) running at 0.6 mL/min. The RID signal was analyzed by data processing software (Clarity Lite v. 7.4.1.88 software, DataApex, Prague, Czech Republic). The levels of 5-ALA and PBG in the cell-free medium were assessed using a modified Ehrlich's reagent assay [25]. Porphyrins were analyzed using an HPLC (2690 separation module, Waters™, Milford, MA, USA) equipped with a photodiode array (2996 PDA detector, Waters™, Milford, MA, USA) detector and a chromatographic column (Chromolith® HighResolution RP-18 endcapped, Supelco, Darmstadt, Germany). The UV absorbance was detected at 400 nm and data were processed using Empower 3 software (Waters™, Milford, MA, USA). A mobile-phase system previously outlined [26] was used with minor modifications. Briefly, the mobile phase consisted of two solvent mixtures: solvent A (7.7 g/L ammonium acetate, 125 mL/L acetonitrile, adjusted to pH 5.17 with glacial acetic acid) and solvent B (a methanol-glacial acetic acid mixture with a volume ratio at 10:1). The flow rate of the mobile phase was 1 mL/min. An isocratic elution step was used with 100% solvent A for 5 min, followed by a linear gradient from 0 to 100% solvent B over 30 min, and further followed by 100% solvent B for 5 min. The column temperature was maintained at 45 °C. The CP percentage yield was determined by calculating the ratio of the produced CP to the maximum theoretical CP production based on the consumed glycerol. This calculation assumed a one-to-sixteen molar ratio, meaning 1 mole of CP was produced for every 16 moles of glycerol consumed.

3. Results

3.1. Effects of the Native HemD for CP Biosynthesis

Our previous study [20] showed that heterologous coexpression of *hemA* from *Rhodobacter sphaeroides* and the native *hemB* can increase the metabolic flux into the Shemin/C4 pathway, resulting in enhanced UP biosynthesis with significant culture pigmentation. On the other hand, the inclusion of the native *hemC* for coexpression was detrimental to porphyrin biosynthesis and even completely blocked the culture pigmentation. To investigate the effects of the native HemD on CP biosynthesis, we derived a plasmid pK-hemABD by heterologous coexpression of *hemA* from *R. sphaeroides* and *hemB/D* from *E. coli* in CPC-SbmΔ*iclR*Δ*sdhA*, resulting in BA001. For effective coexpression, the three genes of *hemA*, *hemB*, and *hemD* were cloned to form an operon regulated by the strong *trc* promoter and each gene had an individual strong RBS. The increased *hemD* expression could presumably direct more carbon flux toward the classical heme-biosynthetic pathway by enhancing the specific conversion of hydroxymethylbilane (HMB) to Uroporphyrinogen III (UPG-III) (Figure 1), rather than Uroporphyrinogen I (UPG-I) which occurs via autoxidation. We also supplemented all the cultures with 2 g/L glycine to ensure that porphyrin biosynthesis was not limited by glycine availability. For an abundant supply of succinyl-CoA for porphyrin biosynthesis, the production host with a double mutation of Δ*iclR*Δ*sdhA* was used and all CP-producing strains were cultivated aerobically [27].

Cultivation of BA001 showed normal cell growth with rapid glycerol consumption and significant acetogenesis (Figure 2A). Notably, BA001 produced high levels of 5-ALA and PBG, peaking at 257.7 mg/L (19.6 mg/OD₆₀₀/L) and 1472 mg/L (112 mg/OD₆₀₀/L) at 57 h, respectively (Figure 2B). This strain also exhibited significant pigmentation, producing 430.7 mg/L (2.55% yield) UP-I and 363 mg/L (2.2% yield) UP-III, respectively (Figure 2C,D). The results suggest that overexpression of *hemA/B/D* primarily led to UP production, but hardly any CP.

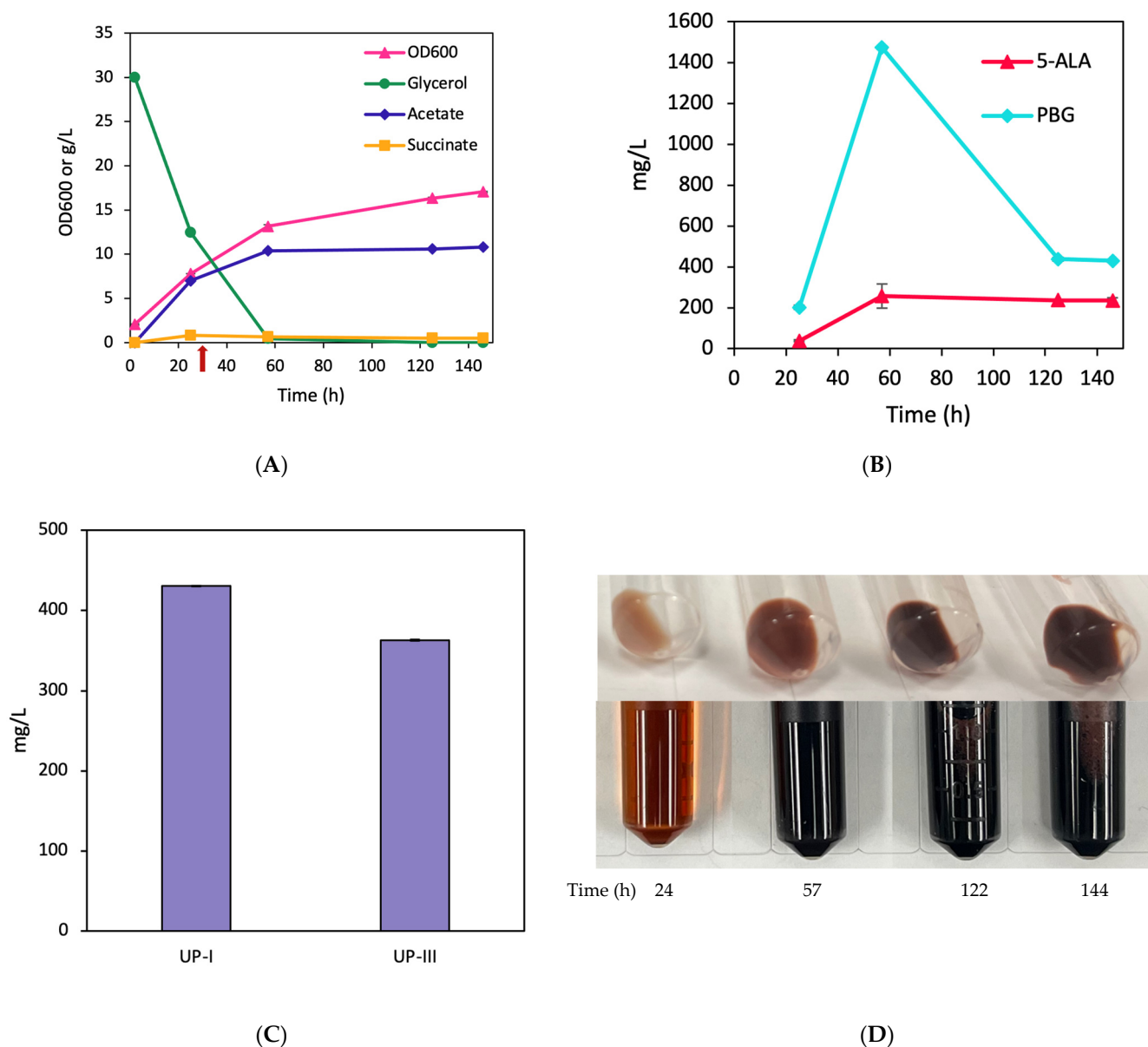


Figure 2. Aerobic bioreactor cultivation of BA001 for porphyrin biosynthesis. Time profiles of (A) cell density (OD_{600}), glycerol consumption, and acetate/succinate formation (the red arrow shows glycine supplementation), (B) 5-ALA and PBG biosynthesis, and (C) UP biosynthesis. (D) Image of CFM and cell paste samples at different time points. All values are reported as means \pm SD ($n = 2$).

3.2. Effects of the Native HemD/E for CP Biosynthesis

To investigate the effects of the native *hemD/E* on CP biosynthesis, we derived a CP-producing strain, BA002, by heterologous coexpression of *hemA* from *R. sphaeroides* and *hemB/D/E* from *E. coli*. For effective coexpression, the four genes of *hemA*, *hemB*, *hemD*, and *hemE* were cloned in a single plasmid to generate pK-hemABD-E, where the *hemA/B/D* genes formed the first operon regulated by the strong *trc* promoter, *hemE* formed the second operon regulated by the strong *gracmax* promoter, and each gene had an individual strong RBS.

Cultivation of BA002 showed normal cell growth with rapid glycerol consumption and significant acetogenesis (Figure 3A). The strain produced 5-ALA and PBG, with peak levels of 99.7 mg/L (5.4 mg/ OD_{600} /L) and 665.7 mg/L (35.7 mg/ OD_{600} /L), respectively (Figure 3B). Additionally, the BA002 culture had intensified pigmentation, producing 84.3 mg/L (0.6% yield) and 182.1 mg/L (1.4% yield) of CP-I and CP-III, respectively

(Figure 3C,D), with 17.5 mg/L and 20.1 mg/L of UP-I and UP-III being produced as side products, respectively (Figure 3C). The results suggest that a higher expression level of the native HemE was critical for CP production.

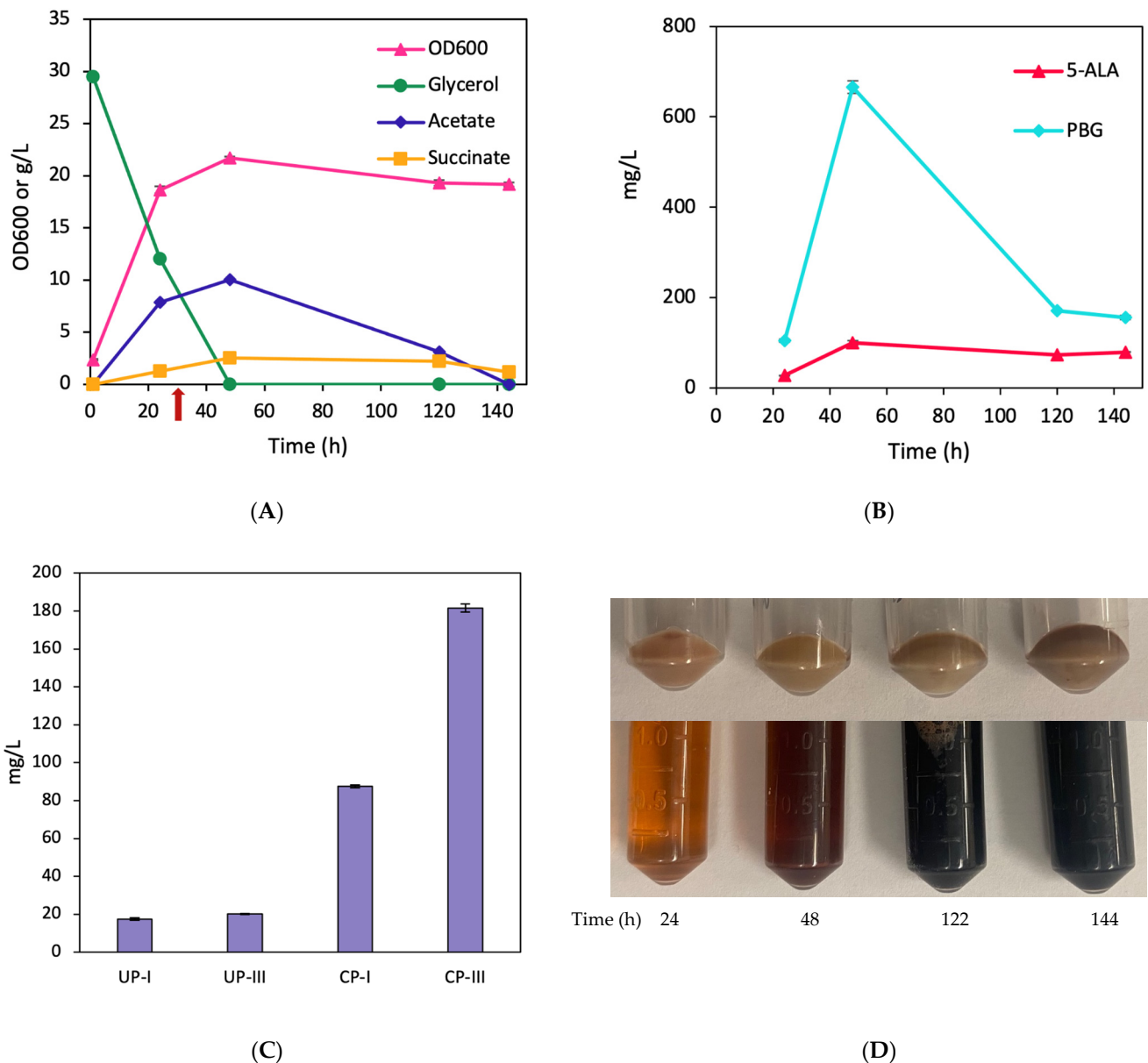


Figure 3. Aerobic bioreactor cultivation of BA002 for porphyrin biosynthesis. Time profiles of (A) cell density (OD_{600}), glycerol consumption, and acetate/succinate formation (the red arrow shows glycine supplementation), (B) 5-ALA and PBG biosynthesis, and (C) CP biosynthesis. (D) Image of CFM and cell paste samples at different time points. All values are reported as means \pm SD ($n = 2$).

3.3. Tuning of Expression Levels of HemD/E for CP Biosynthesis

To further evaluate the effect of *hemD/E* on CP biosynthesis, we constructed another plasmid pK-hemAB-DE, in which the two genes, *hemA/B*, were in the first operon regulated by the *trc* promoter and *hemD/E* were in the second operon regulated by the *gracmax* promoter, resulting in CP-producing strain BA003. Such designs can potentially lead to a higher expression level of *hemD* and a lower expression level of *hemE*, in comparison to pK-hemABD-E. The tuning of the expression levels of the key enzymes in the Shemin/C4 pathway can potentially enable the identification of the step(s) limiting the overall CP biosynthesis.

Similar to BA002, cultivation of BA003 displayed a significant pigmentation (Figure 4D) but cell growth was somewhat retarded with significant acetogenesis (Figure 4A). Also, BA003 exhibited a similar pattern in the production of 5-ALA and PBG in comparison to BA002, with peak levels of 93 mg/L (10 mg/OD₆₀₀/L) and 867 mg/L (92.7 mg/OD₆₀₀/L), respectively (Figure 4B). Nevertheless, BA003 produced CP-I and CP-III slightly less than BA002, peaking at 68.2 mg/L (0.51% yield) and 119 mg/L (0.89% yield), respectively (Figure 4C). In addition, 18.6 mg/L UP-I and 20.3 mg/L UP-III were also produced. These observations further suggest the importance of the expression level of the native HemE for CP biosynthesis.

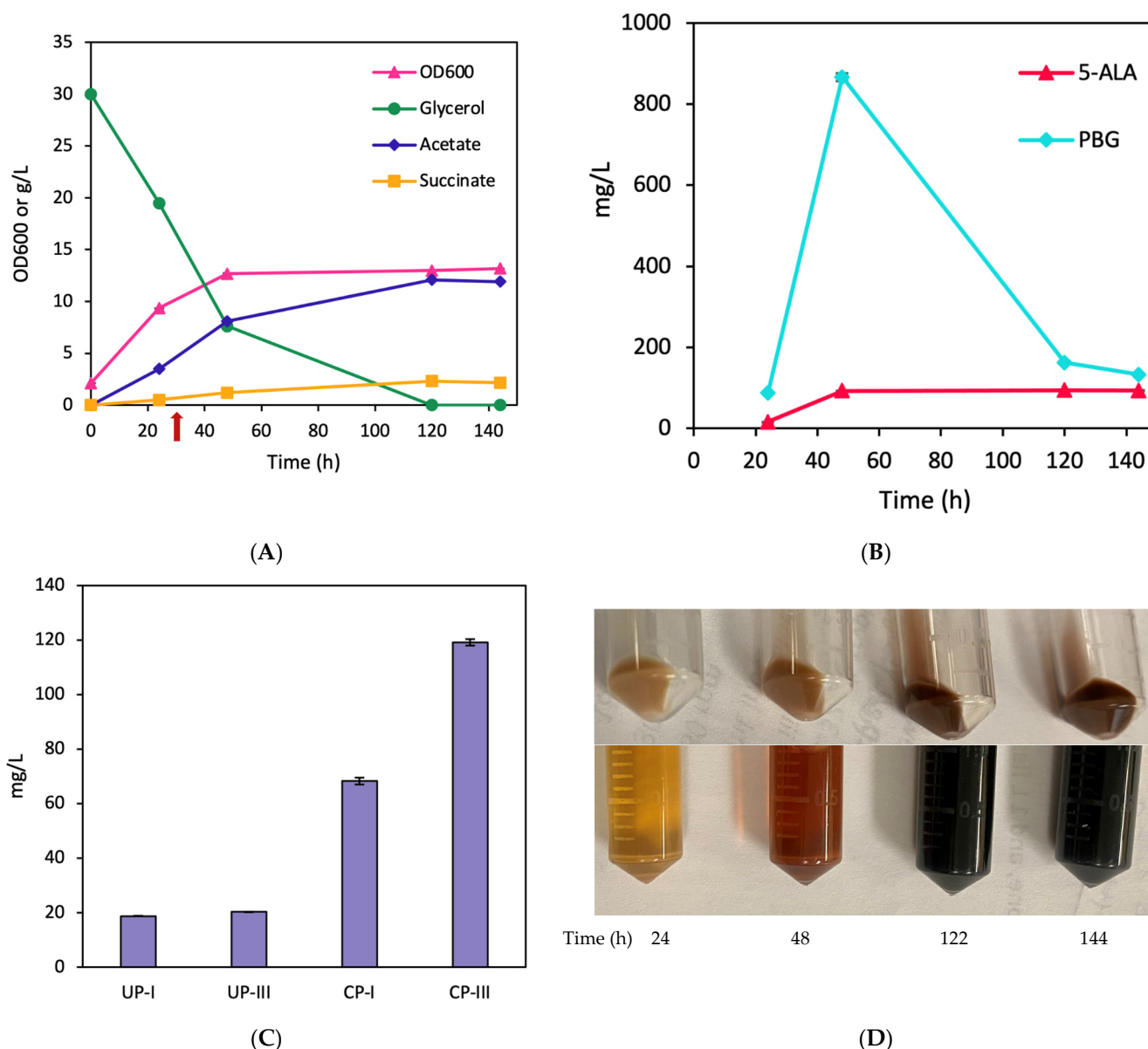


Figure 4. Aerobic bioreactor cultivation of BA003 for porphyrin biosynthesis. Time profiles of (A) cell density (OD₆₀₀), glycerol consumption, and acetate/succinate formation (the red arrow shows glycine supplementation), (B) 5-ALA and PBG biosynthesis, and (C) CP biosynthesis. (D) Image of CFM and cell paste samples at different time points. All values are reported as means ± SD (n = 2).

3.4. Effects of HemY on CP Biosynthesis

The enzymatic conversion of CPG-III to CP-III is mediated by HemY (Figure 1). To investigate the effects of *hemY* on CP biosynthesis, we derived two plasmids, pK-hemABD-

EY_{B,S} and pK-hemABD-EY, by overexpressing *hemA/B/D* in the first operon regulated by *trc* promoter and overexpressing *hemE* and *hemY* from either *B. subtilis* or *E. coli* in the second operon regulated by *gracmax* promoter, resulting in the CP-producing strains BA004 and BA005.

Upon cultivation of BA004, we observed a reduced pigmentation (Figure 5D) though cells grew normally with similar acetogenesis to BA002 and more rapid consumption of glycerol (Figure 5A). Also, BA004 exhibited reduced 5-ALA and PBG production in comparison to BA002, with peak levels of 104 mg/L (8.4 mg/OD₆₀₀/L) and 207 mg/L (16.7 mg/OD₆₀₀/L) at 120 h, respectively (Figure 5B). As a result, BA004 produced significantly less CP-I and CP-III than BA002, with peak concentrations reaching only 43.8 mg/L (0.33% yield) and 62.2 mg/L (0.47% yield), respectively. In addition, 6.2 mg/L and 10.6 mg/L of UP-I and UP-III were produced as side products, respectively (Figure 5C).

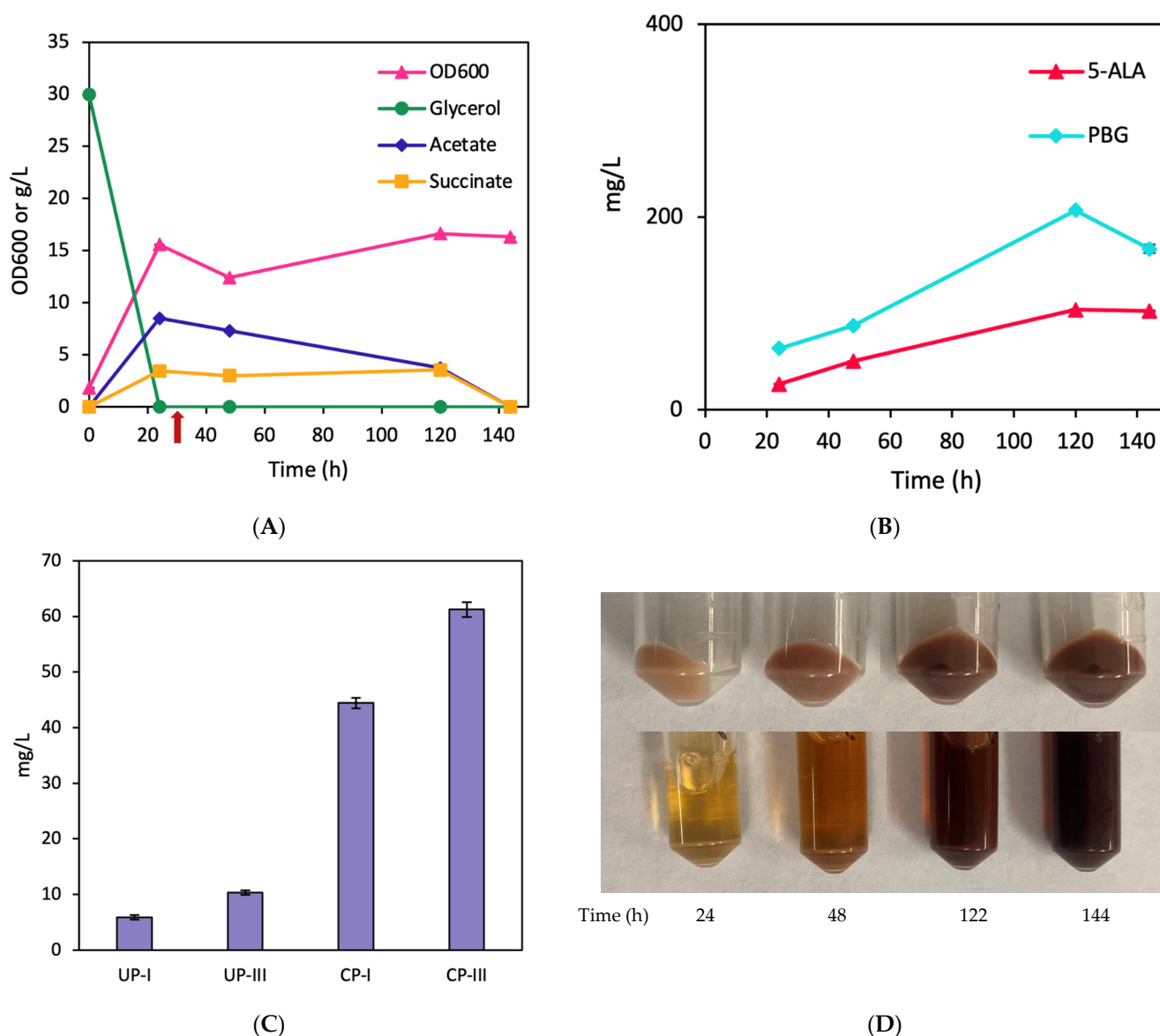


Figure 5. Aerobic bioreactor cultivation of BA004 for porphyrin biosynthesis. Time profiles of (A) cell density (OD₆₀₀), glycerol consumption, and acetate/succinate formation (the red arrow shows glycine supplementation), (B) 5-ALA and PBG biosynthesis, and (C) CP biosynthesis. (D) Image of CFM and cell paste samples at different time points. All values are reported as means ± SD (n = 2).

Similarly, a reduced pigmentation was observed in cultivation of BA005 (Figure 6D) though cells grew normally with similar acetogenesis to BA002 (Figure 6A). Additionally, BA005 exhibited reduced 5-ALA and PBG production in comparison to BA002, with peak levels of 52.7 mg/L (3.7 mg/OD₆₀₀/L) and 60.4 mg/L (4.2 mg/OD₆₀₀/L) at 144 h, respectively (Figure 6B). As a result, BA005 yielded significantly lower amounts of CP-I and CP-III compared to BA002, with peak concentrations of 61.1 mg/L (0.46% yield) and 47.2 mg/L (0.35% yield), respectively. In addition, 5.8 mg/L and 6.2 mg/L of UP-I and UP-III were produced as side products, respectively. (Figure 6C). These observations suggest adverse effects upon *hemY* overexpression for CP biosynthesis. Consequently, we excluded *hemY* for coexpression in the subsequent experiments.

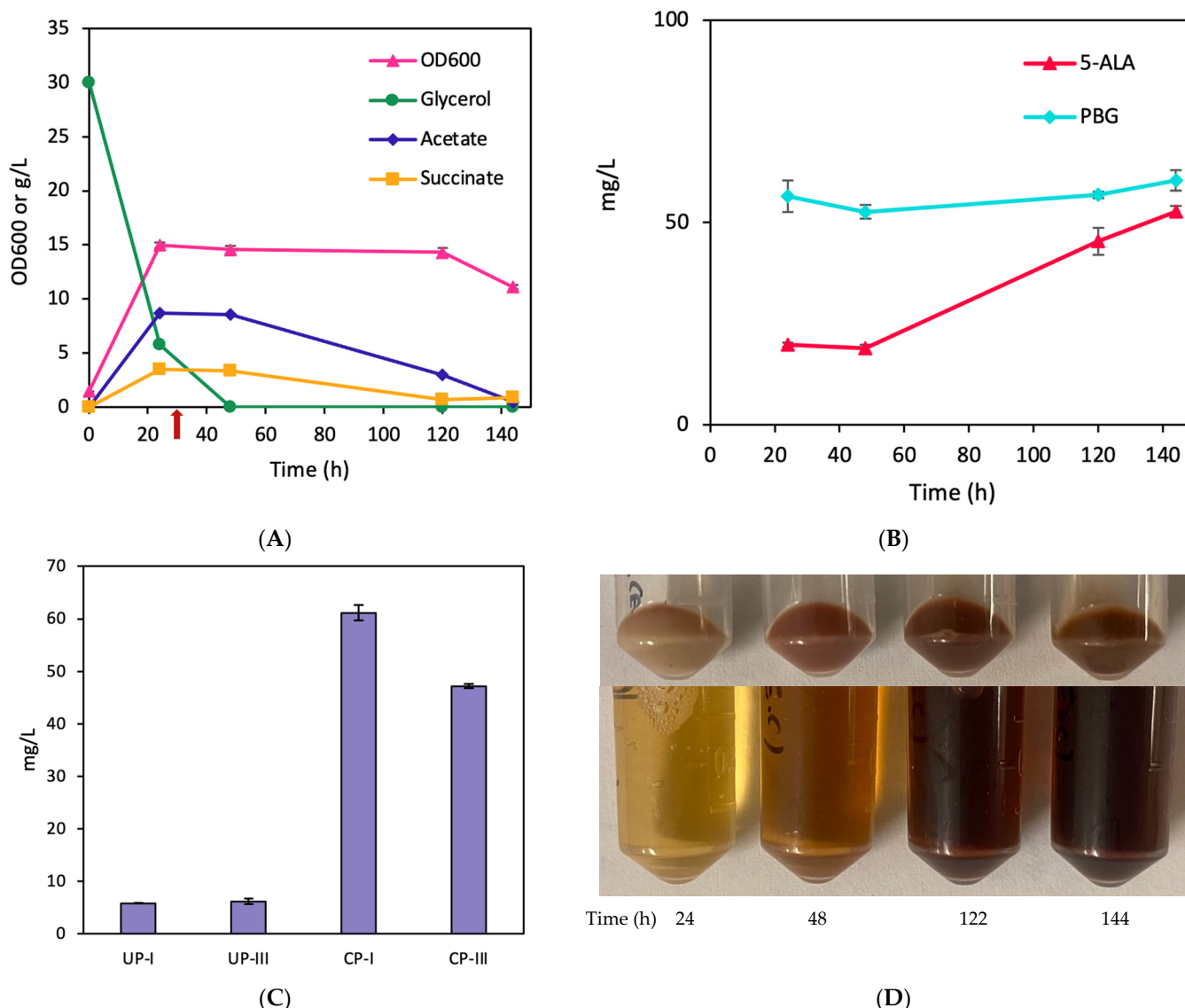


Figure 6. Aerobic bioreactor cultivation of BA005 for porphyrin biosynthesis. Time profiles of (A) cell density (OD₆₀₀), glycerol consumption, and acetate/succinate formation (the red arrow shows glycine supplementation), (B) 5-ALA and PBG biosynthesis, and (C) CP biosynthesis. (D) Image of CFM and cell paste samples at different time points. All values are reported as means ± SD (n = 2).

3.5. HemD Overexpression Was Not Essential for CP Biosynthesis

Based on the cultivation results of BA002 and BA003, we further investigated whether the overexpression of the native *hemD* was essential for CP biosynthesis. To do this, we excluded *hemD* in the next derived plasmid pK-hemAB-E by overexpressing *hemA/B* in the

first operon regulated by the *trc* promoter and *hemE* in the second operon regulated by the *gracmax* promoter, resulting in the CP-producing strain BA006.

BA006 exhibited a glycerol consumption rate similar to BA002, accompanied by a progressively increasing cell density and significant acetogenesis (Figure 7A). Notably, BA006 produced high levels of 5-ALA and PBG, peaking at 408 mg/L (36.9 mg/OD₆₀₀/L) and 1156 mg/L (104.6 mg/OD₆₀₀/L) at 48 h, respectively (Figure 7B). Most importantly, BA006 produced even more CP than BA002 with a total titer of 353 mg/L comprising 102.4 mg/L and 250.6 mg/L of CP-I and CP-III, respectively (0.77% and 1.88% yields) (Figure 7C,D). Also, note that the product ratio/distribution of CP-I and CP-III in BA006 was similar to BA002, suggesting that *hemD* overexpression did not change the metabolic flux distribution between the classical pathway and autoxidation pathway at the node of HMB. Finally, it is noteworthy that other porphyrins were not detected as side products in this cultivation.

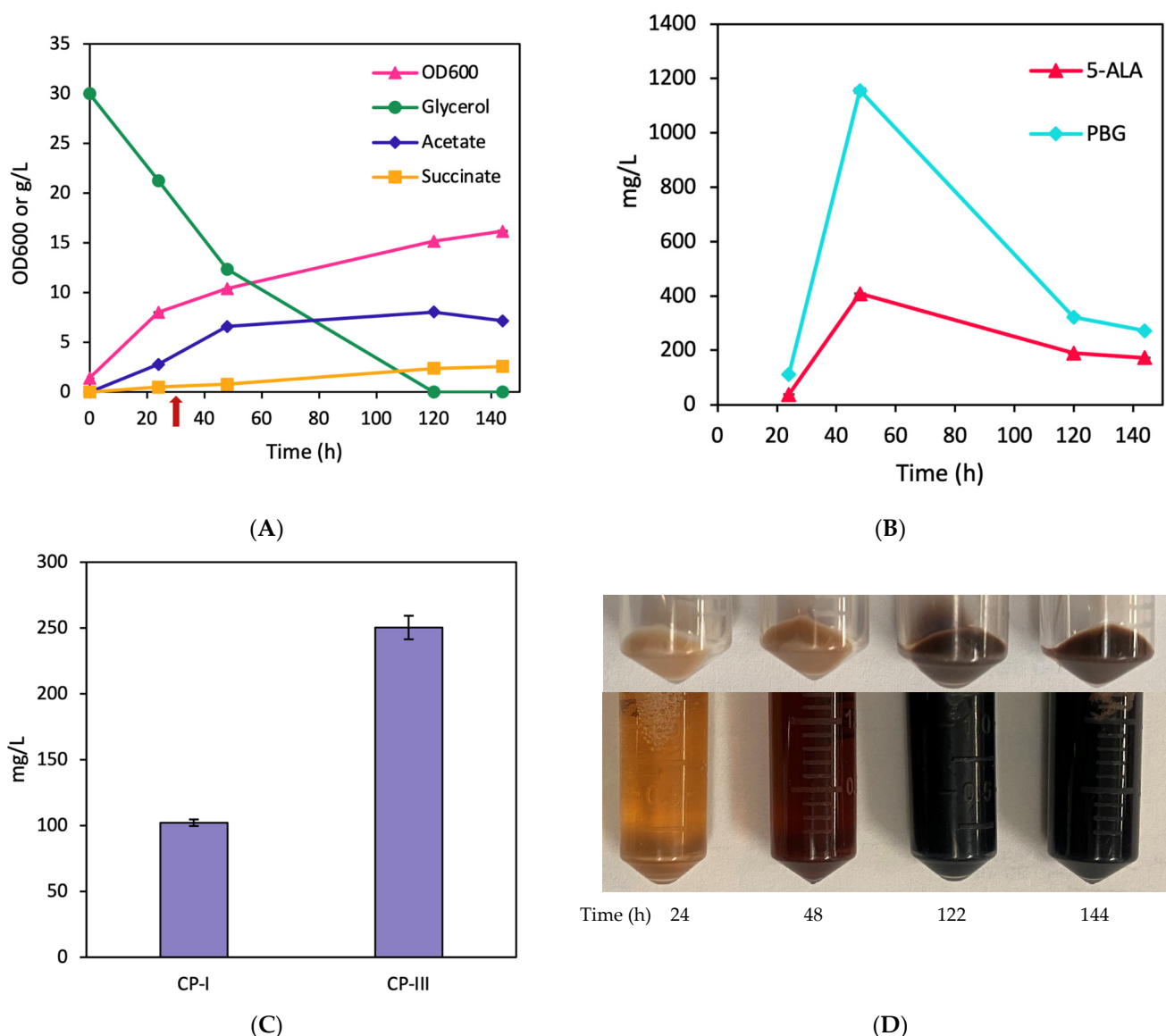


Figure 7. Aerobic bioreactor cultivation of BA006 for porphyrin biosynthesis. Time profiles of (A) cell density (OD₆₀₀), glycerol consumption, and acetate/succinate formation (the red arrow shows glycine supplementation), (B) 5-ALA and PBG biosynthesis, and (C) CP biosynthesis. (D) Image of CFM and cell paste samples at different time points. All values are reported as means ± SD (n = 2).

4. Discussion

In this study, we enhanced CP biosynthesis in *E. coli* by strategically implementing and manipulating the Shemin/C4 pathway. In the production host with a double mutation of $\Delta iclR\Delta sdhA$ [27], the carbon flux from the tricarboxylic acid (TCA) cycle was redirected toward succinyl-CoA, a critical precursor in the CP biosynthesis pathway. Such redirection of carbon flux not only provided an abundant supply of succinyl-CoA but also enabled CP biosynthesis under aerobic conditions. The implementation of the Shemin/C4 pathway into the host strain was achieved through the heterologous expression of *hemA* from *R. sphaeroides*. Among the six genes, i.e., *hemA/B/C/D/E/Y*, contributing to CP biosynthesis (Figure 1), we previously identified the importance of *hemA/B* overexpression for UP biosynthesis, suggesting that the overall porphyrin biosynthesis via the Shemin/C4 pathway could be potentially limited by the two steps converting succinyl-CoA and glycine to PBG. In addition, we previously observed that the genomic expression level of *hemC* was sufficient for effective UP biosynthesis and *hemC* overexpression could potentially disrupt the metabolic activity of the Shemin/C4 pathway, resulting in the complete disappearance of culture pigmentation [20]. Additionally, prior studies have demonstrated that downregulation of *hemC* can result in extracellular accumulation of PBG [28]. Hence, in this study, *hemA/B* were included whereas *hemC* was excluded for overexpression in all the engineered strains for CP biosynthesis.

To evaluate the effects of the other three hem-genes, i.e., *hemD/E/Y*, on CP biosynthesis, we first derived strain BA001 by overexpressing *hemA/B/D*. Cultivation of BA001 revealed substantial pigmentation with extracellular production of UP (both UP-I and UP-III) only. Note that we previously observed that *hemD* overexpression hardly affected UP biosynthesis, suggesting that the genomic expression level of *hemD* was sufficient to drive the conversion of HBM to UPG-III. The absence of CP biosynthesis in BA001 also indicated a potential limitation in the reactions downstream of CPG-III catalyzed by HemE/Y. Specifically, HemE, which is responsible for catalyzing the conversion of UPG-III to CPG-III, can potentially play a critical role in the overall CP biosynthesis.

In the next attempt, we overexpressed the *hemA/B/D/E* genes from the plasmid pK-hemABD-E in BA002. Cultivation of BA002 resulted in a significant pigmentation with extracellular production of CP (both CP-I and CP-III), suggesting the critical role of HemE for CP biosynthesis. The produced CP can be extracellularly secreted, posing minimal intracellular toxicity on cell physiology. The production of UP-I in BA001 and CP-I in BA002 indicates the involvement of autooxidation as a side reaction converting HMB to UPG-I in *E. coli*. The relatively high titer ratio of UP-I/UP-III at 1.19 in BA001 suggests that conversion of HMB was more favorable to UPG-I via autooxidation than UPG-III via HemD (even though *hemD* was overexpressed). The observation was unsurprising since bacterial cultivation for porphyrin production was conducted aerobically. However, such carbon flux distribution appears to be reversed, i.e., conversion of HMB was more favorable to UPG-III/CPG-III than UPG-I/CPG-I when *hemE* was also included for overexpression in BA002, even though bacterial cultivation was still conducted aerobically. Note that the total porphyrin titer in BA002 was significantly reduced compared to BA001 for unknown reasons. Nevertheless, the results suggest that the overexpressed HemE could play a critical role by directing more carbon flux toward the classical Shemin/C4 pathway for CP-III biosynthesis in *E. coli*. Also, it appears that more UPG-I was converted to CPG-I, resulting in increased CP-I titer in BA002. The results suggest that HemE can potentially mediate the conversion of UPG-I to CPG-I in a similar mechanism to its native activity converting UPG-III to CPG-III.

For overexpressing *hemA/B/D/E*, we also made another plasmid pK-hemAB-DE in which *hemD/E* genes were fused to form the second operon whose expression was regulated by the *gracmax* promoter, resulting in another engineered strain BA003. Compared to the plasmid pK-hemABD-E (in BA002), in which *hemE* was the only gene in the second operon regulated by the *gracmax* promoter, *hemE* expression for pK-hemAB-DE would presumably be lower whereas *hemD* expression for pK-hemAB-DE would be higher. The

upregulated *hemD* expression and downregulated *hemE* expression for pK-hemAB-DE can be attributed to the transcription process for a gene operon, resulting in the formation of multiple immature cistronic mRNAs with the first mRNA being more stable than the latter mRNA(s) [29,30]. Compared to BA002, we observed a slight reduction in CP biosynthesis with a similar titer ratio of CP-III/CP-I upon cultivation of BA003. The reduced CP biosynthesis may be associated with the reduced expression level of *hemE* in BA003.

Next, we investigated the effects of the final step on CP biosynthesis, i.e., the conversion of coproporphyrinogen III (CPG-III) into CP-III, which is catalyzed by HemY. To do this, we included *B. subtilis hemY* and native *E. coli hemY* for heterologous expression in BA004 and BA005, respectively. Unexpectedly, we noted significantly reduced culture pigmentation and CP titers for both engineered strains. Our observations align with a prior report [26], in which adverse effects of *B. subtilis hemY* overexpression on porphyrin titers were observed in multiple instances. The results suggest a possible inhibitory effect of HemY on the earlier enzymatic conversions for CP biosynthesis. In the CPD pathway of actinobacteria or firmicutes, coproporphyrinogen III oxidase (HemY) primarily catalyzes the oxidation of CPG-III to CP-III, which is a heme precursor unique to the CPD pathway [31]. However, HemY in *E. coli* is often annotated as a protoporphyrinogen oxidase gene, whose biological activity is different from the protoporphyrinogen oxidase found in actinobacteria and firmicutes, and its role in heme biosynthesis is yet to be demonstrated [32]. Although *E. coli* possesses porphyrinogen peroxidase (YfeX), which can also convert CPG-III to CP-III [33], HemY from actinobacteria or firmicutes was identified to be highly efficient for such conversion [4].

Based on the cultivation results of BA001, BA002, and BA003, it appears that increasing *hemD* expression did not contribute to CP biosynthesis. Hence, we decided to exclude *hemD* from the next plasmid construct pK-hemAB-E in BA006. Compared to BA002 and BA003, cultivation of BA006 resulted in a substantial increase in the overall CP production with a more favorable CP-III/CP-I distribution. Interestingly, the conversion of HMB to UPG-III was significantly enhanced by *hemE* overexpression, even in the absence of *hemD* coexpression. The results corroborate the critical role that the overexpressed HemE played in directing more carbon flux toward the classical Shemin/C4 pathway for enhanced CP-III (with minimal UP) biosynthesis. This was particularly important for our developed engineered strains (which were cultivated aerobically) in terms of directing dissimilated carbon flux away from several autooxidations which lead to various side products (such as UP-I, CP-I, and UP-III). Note that cultivation of BA006 only produced CP without detectable UP formation and with considerably reduced acetogenesis compared to the other strains. The results also support our previous observation [20] that the genomic expression level of *hemD* was sufficient enough to maintain the overall metabolic activity of the Shemin/C4 pathway, even under various genetic backgrounds and cultivation conditions for enhanced production of UP and CP. Based on the results of this study, it appears that HemE is the sole enzyme (after the HMB node) critically limiting the overall CP biosynthesis in *E. coli*.

It is notable that we observed significant acetogenesis, reaching up to 10.8 g/L, alongside CP production. Interestingly, in strains like BA002, BA004, and BA005, acetate was eventually metabolized by the cells as a secondary carbon source, particularly once the initial carbon source (i.e., glycerol) was depleted. Achieving complete elimination of acetogenesis during aerobic cultivation of *E. coli* can be particularly challenging due to metabolic constraints linked to carbon overflow metabolism. In conclusion, this study presents a significant advancement in the bio-based production of CP using *E. coli* as a production host, achieving high-level CP production with minimal byproduct formation. Future research could focus on the underlying reason behind the adverse effects of HemY on CP biosynthesis, providing valuable insights into the possible interactions of the pathway enzymes. Additionally, exploring the metabolic pathways and regulatory mechanisms of acetogenesis under aerobic conditions may uncover strategies to mitigate acetate overflow and enhance CP production efficiency.

Supplementary Materials: The following supporting information can be downloaded at: <https://www.mdpi.com/article/10.3390/fermentation10050250/s1>, Table S1. Oligomers used in this study.

Author Contributions: Conceptualization, B.A. and C.P.C.; Methodology, B.A.; Validation, Y.L. and C.P.C.; Formal Analysis, B.A.; Investigation, B.A.; Data Curation, B.A.; Writing—Original Draft, B.A.; Writing—Review and Editing, B.A., A.W., Y.L. and C.P.C.; Supervision, C.P.C.; Funding Acquisition, M.M.-Y. and C.P.C. All authors have read and agreed to the published version of the manuscript.

Funding: This research was funded by the Natural Sciences and Engineering Research Council (NSERC) grant number RGPIN-2019-04611.

Data Availability Statement: Data are contained within the article and Supplementary Materials.

Conflicts of Interest: The authors declare that they have no known competing financial interests or personal relationships that could have appeared to influence the work reported in this paper. However, portions of the reported data were also included in a US patent application.

References

1. Poulos, T.L. Heme enzyme structure and function. *Chem. Rev.* **2014**, *114*, 3919–3962. [[CrossRef](#)] [[PubMed](#)]
2. Beas, J.Z.; Videira, M.A.; Saraiva, L.M. Regulation of bacterial haem biosynthesis. *Coord. Chem. Rev.* **2022**, *452*, 214286. [[CrossRef](#)]
3. Celis, A.I.; DuBois, J.L. Making and breaking heme. *Curr. Opin. Struct. Biol.* **2019**, *59*, 19–28. [[CrossRef](#)] [[PubMed](#)]
4. Dailey, H.A.; Dailey, T.A.; Gerdes, S.; Jahn, D.; Jahn, M.; O'Brian, M.R.; Warren, M.J. Prokaryotic heme biosynthesis: Multiple pathways to a common essential product. *Microbiol. Mol. Biol. Rev.* **2017**, *81*, e00048-16. [[CrossRef](#)] [[PubMed](#)]
5. Kořený, L.; Oborník, M.; Horáková, E.; Waller, R.F.; Lukeš, J. The convoluted history of haem biosynthesis. *Biol. Rev.* **2022**, *97*, 141–162. [[CrossRef](#)] [[PubMed](#)]
6. Phillips, J.D. Heme biosynthesis and the porphyrias. *Mol. Genet. Metab.* **2019**, *128*, 164–177. [[CrossRef](#)]
7. Aman Mohammadi, M.; Ahangari, H.; Mousazadeh, S.; Hosseini, S.M.; Dufossé, L. Microbial pigments as an alternative to synthetic dyes and food additives: A brief review of recent studies. *Bioprocess Biosyst. Eng.* **2022**, *45*, 1–12. [[CrossRef](#)] [[PubMed](#)]
8. Qin, Z.; Wang, X.; Gao, S.; Li, D.; Zhou, J. Production of Natural Pigments Using Microorganisms. *J. Agric. Food Chem.* **2023**, *71*, 9243–9254. [[CrossRef](#)] [[PubMed](#)]
9. Yang, D.; Park, S.Y.; Park, Y.S.; Eun, H.; Lee, S.Y. Metabolic engineering of *Escherichia coli* for natural product biosynthesis. *Trends Biotechnol.* **2020**, *38*, 745–765. [[CrossRef](#)]
10. Frankenberg, N.; Moser, J.; Jahn, D. Bacterial heme biosynthesis and its biotechnological application. *Appl. Microbiol. Biotechnol.* **2003**, *63*, 115–127. [[CrossRef](#)]
11. Anzaldi, L.L.; Skaar, E.P. Overcoming the heme paradox: Heme toxicity and tolerance in bacterial pathogens. *Infect. Immun.* **2010**, *78*, 4977–4989. [[CrossRef](#)] [[PubMed](#)]
12. Su, H.; Chen, X.; Chen, S.; Guo, M.; Liu, H. Applications of the whole-cell system in the efficient biosynthesis of heme. *Int. J. Mol. Sci.* **2023**, *24*, 8384. [[CrossRef](#)] [[PubMed](#)]
13. Layer, G. Heme biosynthesis in prokaryotes. *Biochim. Et Biophys. Acta BBA-Mol. Cell Res.* **2021**, *1868*, 118861. [[CrossRef](#)] [[PubMed](#)]
14. Di Pierro, E.; De Canio, M.; Mercadante, R.; Savino, M.; Granata, F.; Tavazzi, D.; Nicolli, A.M.; Trevisan, A.; Marchini, S.; Fustinoni, S. Laboratory diagnosis of porphyria. *Diagnostics* **2021**, *11*, 1343. [[CrossRef](#)]
15. Neuvonen, M.; Tornio, A.; Hirvensalo, P.; Backman, J.T.; Niemi, M. Performance of plasma coproporphyrin I and III as OATP1B1 biomarkers in humans. *Clin. Pharmacol. Ther.* **2021**, *110*, 1622–1632. [[CrossRef](#)] [[PubMed](#)]
16. Al-Hussaini, A.; Asery, A.; Alharbi, O. Urinary coproporphyrins as a diagnostic biomarker of Dubin-Johnson syndrome in neonates: A diagnostic pathway is proposed. *Saudi J. Gastroenterol.* **2023**, *29*, 183–190. [[CrossRef](#)] [[PubMed](#)]
17. Belousova, I.; Dobrun, M.; Galebskaya, L.; Gorelov, S.; Kislyakov, I.; Kolbasov, S.; Kris'ko, A.; Kris'ko, T.; Malkov, M.; Murav'eva, T. New preparation based on coproporphyrin III for photoluminescence diagnostics and photodynamic therapy. In Proceedings of the Laser Optics 2010, St Petersburg, Russia, 28 June–2 July 2010; pp. 200–205.
18. Gilibili, R.R.; Chatterjee, S.; Bagul, P.; Mosure, K.W.; Murali, B.V.; Mariappan, T.T.; Mandlekar, S.; Lai, Y. Coproporphyrin-I: A fluorescent, endogenous optimal probe substrate for ABCC2 (MRP2) suitable for vesicle-based MRP2 inhibition assay. *Drug Metab. Dispos.* **2017**, *45*, 604–611. [[CrossRef](#)]
19. Walter, A.B.; Simpson, J.; Jenkins, J.L.; Skaar, E.P.; Jansen, E.D. Optimization of optical parameters for improved photodynamic therapy of *Staphylococcus aureus* using endogenous coproporphyrin III. *Photodiagnosis Photodyn. Ther.* **2020**, *29*, 101624. [[CrossRef](#)] [[PubMed](#)]
20. Arab, B.; Westbrook, A.W.; Moo-Young, M.; Liu, Y.; Chou, C.P. Bio-Based Production of Uroporphyrin in *Escherichia coli*. *Synth. Biol. Eng.* **2024**, *2*, 10002. [[CrossRef](#)]
21. Jones, J.A.; Koffas, M.A. Optimizing metabolic pathways for the improved production of natural products. In *Methods in Enzymology*; Elsevier: Amsterdam, The Netherlands, 2016; Volume 575, pp. 179–193.
22. Miscevic, D.; Mao, J.Y.; Moo-Young, M.; Chou, C.H.P. High-level heterologous production of propionate in engineered *Escherichia coli*. *Biotechnol. Bioeng.* **2020**, *117*, 1304–1315. [[CrossRef](#)]

23. Srirangan, K.; Liu, X.; Westbrook, A.; Akawi, L.; Pyne, M.E.; Moo-Young, M.; Chou, C.P. Biochemical, genetic, and metabolic engineering strategies to enhance coproduction of 1-propanol and ethanol in engineered *Escherichia coli*. *Appl. Microbiol. Biotechnol.* **2014**, *98*, 9499–9515. [[CrossRef](#)] [[PubMed](#)]
24. Gibson, D.G.; Young, L.; Chuang, R.-Y.; Venter, J.C.; Hutchison, C.A.; Smith, H.O. Enzymatic assembly of DNA molecules up to several hundred kilobases. *Nat. Methods* **2009**, *6*, 343–345. [[CrossRef](#)] [[PubMed](#)]
25. Mauzerall, D.; Granick, S. The Occurrence and Determination of Δ -Aminolevulinic Acid and Porphobilinogen in Urine. *J. Biol. Chem.* **1956**, *219*, 435–446. [[CrossRef](#)] [[PubMed](#)]
26. Kwon, S.J.; De Boer, A.L.; Petri, R.; Schmidt-Dannert, C. High-Level Production of Porphyrins in Metabolically Engineered *Escherichia coli*: Systematic Extension of a Pathway Assembled from Overexpressed Genes Involved in Heme Biosynthesis. *Appl. Environ. Microbiol.* **2003**, *69*, 4875–4883. [[CrossRef](#)]
27. Miscevic, D.; Mao, J.Y.; Kefale, T.; Abedi, D.; Moo-Young, M.; Perry Chou, C. Strain engineering for high-level 5-aminolevulinic acid production in *Escherichia coli*. *Biotechnol Bioeng* **2021**, *118*, 30–42. [[CrossRef](#)]
28. Lall, D.; Miscevic, D.; Bruder, M.; Westbrook, A.; Aucoin, M.; Moo-Young, M.; Perry Chou, C. Strain engineering and bioprocessing strategies for biobased production of porphobilinogen in *Escherichia coli*. *Bioresour. Bioprocess.* **2021**, *8*, 1–16. [[CrossRef](#)]
29. Makoff, A.; Smallwood, A. The use of two-cistron constructions in improving the expression of a heterologous gene in *E. coli*. *Nucleic Acids Res.* **1990**, *18*, 1711–1718. [[CrossRef](#)]
30. Newbury, S.F.; Smith, N.H.; Higgins, C.F. Differential mRNA stability controls relative gene expression within a polycistronic operon. *Cell* **1987**, *51*, 1131–1143. [[CrossRef](#)] [[PubMed](#)]
31. Dailey, H.A.; Gerdes, S.; Dailey, T.A.; Burch, J.S.; Phillips, J.D. Noncanonical coproporphyrin-dependent bacterial heme biosynthesis pathway that does not use protoporphyrin. *Proc. Natl. Acad. Sci. USA* **2015**, *112*, 2210–2215. [[CrossRef](#)]
32. Panek, H.; O'Brian, M.R. A whole genome view of prokaryotic haem biosynthesis. *Microbiology* **2002**, *148*, 2273–2282. [[CrossRef](#)]
33. Dailey, H.A.; Septer, A.N.; Daugherty, L.; Thames, D.; Gerdes, S.; Stabb, E.V.; Dunn, A.K.; Dailey, T.A.; Phillips, J.D. The *Escherichia coli* protein YfeX functions as a porphyrinogen oxidase, not a heme dechelataase. *MBio* **2011**, *2*, e00248-11. [[CrossRef](#)] [[PubMed](#)]

Disclaimer/Publisher's Note: The statements, opinions and data contained in all publications are solely those of the individual author(s) and contributor(s) and not of MDPI and/or the editor(s). MDPI and/or the editor(s) disclaim responsibility for any injury to people or property resulting from any ideas, methods, instructions or products referred to in the content.